Theor Chem Account (2007) 118:579–588
DOI 10.1007/s00214-007-0341-3

REGULAR ARTICLE

Charge-charge and cation-π interactions in ligand binding to G protein-coupled receptors

N. Dölker · X. Deupi · L. Pardo · M. Campillo

Received: 27 January 2007 / Accepted: 7 February 2007 / Published online: 7 June 2007

Abstract To study the importance of charge–charge and cation-π interactions for the binding of positively charged amine ligands to their receptors, the energies of interaction between $[(CH_3)_4–N]^+$, $[(CH_3)_3–NH]^+$, and $[(CH_3)_4–NH_3]^+$ and acetate, as a model of Asp and Glu, and with benzene, as a model of aromatic side chains, were obtained at the MP2/aug-cc-pVDZ level of theory. The free energies of solvation in water were also calculated for the different amines. It was found that, although primary amines form stronger charge–charge interactions with acetate than tertiary or quaternary amines, the difference is not large enough to compensate their higher solvation energy. Quaternary amines show the weakest interaction with acetate. However, their alkyl groups can interact with various aromatic groups, enhancing ligand binding to the receptor. The analysis was completed with MD calculations on amine binding to the G protein-coupled receptors β_2AR and CCR5. The calculations on the model systems were found to be in good agreement with the simulations of the ligand-receptor complexes.

Keywords Cation-π interactions · G protein-coupled receptors · Ligand binding

1 Introduction

Ligand-receptor binding affinity is based on a mutual structural and energetic recognition, where ligands interact with the biological target through ionic, aromatic-aromatic, hydrogen bond, or/and van der Waals interactions [1]. Cation-π interactions, however, in spite of experimental support for their importance ([2], and references within), are relatively underappreciated. This type of interaction can be considered as an attraction between the positive charge of the ligand and the quadrupole moment of the aromatic ring, with electrostatic and non-electrostatic (polarizability of the aromatic ring, donor-acceptor and charge-transfer terms, and dispersion forces) terms [2]. The magnitude of the cation-π interaction is energetically comparable to a hydrogen bond ([3] and references within), and has been extensively reported in diverse biological systems. Statistical analyses of side-chain interactions [4–7] have revealed that the NH groups of Arg, Lys and His have a preference to be located near aromatic side chains. Recently, the analysis of the transferred NOE NMR structure of the $G_t\alpha$ (340–350) peptide bound to photoactivated rhodopsin suggests that the structure is stabilized by a cation-π interaction between the amine of Lys-341 and the aromatic phenyl ring of Phe-350 [8]. Interestingly, the contribution of this interaction to the stability of the receptor-bound structure is reduced by the presence of an adjacent and competing salt-bridge interaction between the amine of Lys-341 and the C-terminal carboxylate of Phe-350 (see below). The interaction of positively charged ligands with protein aromatic residues through cation-π interactions is also an important element of molecular recognition. For instance, the crystal structure of acetylcholine esterase [9] shows that the cationic quaternary amine group of the ligand is in contact with the side chain of the highly conserved Trp-84. Similarly, cation-π interactions are important for ligand binding in the nicotinic acetylcholine receptor (see [6] for a review; [10,11]) and have also been established in the serotonin-gated ion channel, 5-HT_{3A}R [10].

Contribution to the Serafin Fraga Memorial Issue.

N. Dölker · X. Deupi · L. Pardo · M. Campillo (✉)
Laboratori de Medicina Computacional, Unitat de Bioestadística, Facultat de Medicina, Edifici M, Universitat Autònoma de Barcelona, 08193 Bellaterra, Barcelona, Spain
e-mail: Mercedes.Campillo@uab.es

Charge–charge, interactions between ligands and proteins are also key in the process of ligand recognition. In particular, G protein-coupled receptors (GPCRs) possess family-specific negative Asp or Glu amino acids that bind protonated ligands [12]. GPCRs are only a small subset of the human genome (2–3%) [13–15] but it is estimated that around 40% of prescribed drugs act through these receptors [16–18]. In this family of proteins, the interaction between the positively charged ligand with the negatively charged residue seems to be stabilized by specific and conserved aromatic residues. Several experimental and theoretical studies suggest that the protonated group of amines (cannabinoid [19], dopamine D2 [20], delta opioid [21] or muscarinic acetylcholine receptors [22,23]) and peptides (neuropeptide Y [24], neurokinin-1 [25], bombesin peptides [26], neurotensin-1 [27]) is involved in cation-π interactions with specific aromatic residues lining the binding site.

Although many of these works suggest that binding of the positively charged amine group to the receptor may involve the simultaneous interaction with a negative charge and aromatic groups, this ternary system (negative amino acid–positive amine–aromatic amino acid) has not been described in detail. In this paper we aim to describe the influence of the aromatic residues on the ionic ligand-receptor interactions found in GPCRs, in order to learn about its role in the process of ligand recognition.

2 Methods

2.1 Residue numbering scheme

We use a general numbering scheme to identify residues in the transmembrane segments of different GPCRs [28]. Each residue is numbered according to the helix (1–7) in which it is located and to the position relative to the most conserved residue in that helix, arbitrarily assigned to 50. For instance, the most conserved residue in helix 3 is designated with the index number 3.50 ($Arg^{3.50}$), the Asp preceding the Arg is designated $Asp^{3.49}$, and the Tyr following the Arg is designated $Tyr^{3.51}$.

2.2 Quantum chemical calculations

All quantum chemical calculations were carried out using the Gaussian03 package [29]. Geometry optimizations and energy calculations were performed with second order Moller-Plesset perturbation theory (MP2) [30–34] in order to include dispersion forces, highly important in weak electrostatic interactions, such as cation-π complexes. Dunning's correlation corrected aug-cc-pVDZ basis set, as included in the Gaussian03 package [35–39], was used in the calculations. Systems were fully optimized in the gas phase, with the exception of salt-bridge complexes, in which the N–H bond distances in the ammonium compounds were kept frozen at the distances found in the free compounds.

Free energies of solvation in water were calculated at the HF/cc-pVQZ level, using the Polarized Continuum Model [40–45].

2.3 Molecular dynamics simulations

The previously obtained models of the β_2-adrenergic receptor (β_2AR) [46,47] and chemokine CCR5 [48,49], built by homology modeling using the crystal structure of bovine rhodopsin (Protein Data Bank ID code 1GZM [50]) at 2.65 Å of resolution as a template, were employed in the simulations. Transmembrane helix 2 of CCR5 contains the TXP motif that bends the helix [51] and modifies its conformation relative to rhodopsin [48,52]. Structural water molecules 1, 2, 7, 9, and 12 observed in the $D^{2.50}/P^{6.50}/N^{7.49}/Y^{7.53}$ environment of rhodopsin were also included in the models [53]. These water molecules mediate a number of interhelical interactions that are important in maintaining the inactive conformation of the receptor [54–56]. Isoproterenol and dopamine, as ligands of β_2AR, and TAK-779 (see Fig. 1) and the N-terminal domain of the MIP1β peptide (only the APMGSDPP part of the peptide was modeled), as ligands of CCR5, were considered. Isoproterenol, dopamine, and TAK-779 were parameterized with the Antechamber program using the general AMBER force field [57] and HF/6-31G*-derived RESP atomic charges. These ligands were docked in the binding pocket of the receptors according to the experimentally inferred interactions (see Sect. 4). The receptor models with docked ligands were immersed in a patch of pre-equilibrated palmitoyl oleoyl phosphatidyl-choline lipidic bilayer solvated with water. These systems were energy-minimized and then heated to 300 K in 15 ps. This was followed by an equilibration period (15–500 ps) and a production run (500–1,000 ps). The molecular dynamics simulations were carried out with the Sander module of AMBER 9 [58] at constant pressure, using the particle mesh Ewald method and the ff03 force field, SHAKE bond constraints in all bonds, a 2fs integration time step, and constant temperature coupled to a heat bath.

One hundred receptor-ligand structures extracted from the MD trajectories of the production run were used to evaluate free energies of binding using the MM-GBSA methodology, as implemented in the AMBER suite [58] (see [59] or [60] for applications of the MM-GBSA method to the estimation of binding energies).

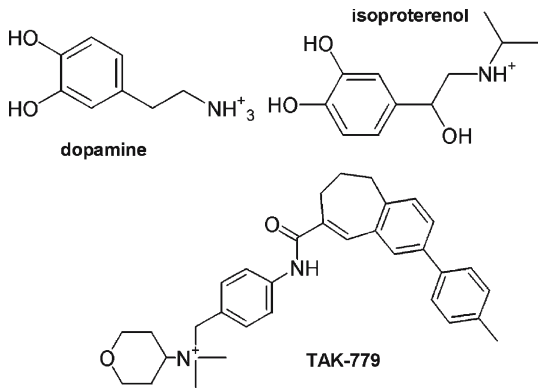

Fig. 1 Chemical structures of β_2AR ligands dopamine and isoproterenol and CCR5 antagonist TAK-779

3 Results

3.1 The model of the protonated amine ligand

The character of the ligands considered in this study varies from fully substituted quaternary to protonated tertiary, secondary and primary amines. Thus, we considered tetramethylammonium $[(CH_3)_4\text{–}N]^+$ (Fig. 2A_1), trimethylammonium $[(CH_3)_3\text{–}NH]^+$(A_2) and methylammonium $[CH_3\text{–}NH_3]^+$ (A_3) as models of these different types of ligands to perform quantum mechanical calculations (see Sect. 2). Fig. 2A_{1-3} shows the optimized geometries as well as the electrostatic potential surfaces of the ligands. It can clearly be seen that, although all three compounds have the same molecular charge, the electrostatic potential is different. The N–H bonds in methylammomium and trimethylammonium are strongly polarized, with important partial positive charges on hydrogen. Tetramethylammonium, on the contrary, shows a more homogeneous charge distribution.

Free energies of solvation in water were also calculated using the Polarizable Continuum Method (see Sect. 2). The results show a clear trend (Table 1): The primary ammonium $[CH_3\text{–}NH_3]^+$ has the highest solvation energy (−65.9 kcal/mol), while methyl addition lowers the value to −49.0 kcal/mol for $[(CH_3)_3 - NH]^+$ and −40.5 kcal/mol for $[(CH_3)_4N]^+$. These differences can be explained by the charge distribution on the amines. The strongly polarized N–H bonds of the primary and tertiary amine lead to a higher solvation energy compared to the less polarized methyl groups of the quaternary amine.

3.2 Charge-charge complexes

The interaction between conserved Glu and Asp residues in the binding site crevice of GPCRs and positively charged amines of the ligand is key in the process of ligand recognition [61]. Thus, we performed quantum mechanical calculations (see Sect. 2) between tetramethylammonium $[(CH_3)_4\text{–}N]^+$, trimethylammonium $[(CH_3)_3\text{–}NH]^+$ and methylammonium $[CH_3\text{–}NH_3]^+$ and acetate $[CH_3 - COO]^-$, as a model of Asp and Glu, to analyze the structural and energetic differences in these charge–charge complexes (Fig. 2B_{1-3}).

In the tetramethylammonium-acetate complex (B_1), which is of Cs symmetry, three of the four nitrogen-bonded methyl groups point towards acetate. Three C–H $\cdots$ O hydrogen bonds are formed with distances of 1.86 and 2.02 Å. The complex formed by trimethylammonium (B_2) shows a similar geometry, with the N–H as well as two methyl groups hydrogen-bonding the carboxylate. The N–H$\cdots$ O bond is quite short (1.52 Å), while the C–H $\cdots$ O bonds are longer than in the case of tetramethylammonium (2.36 Å). Methylammonium, finally, interacts with acetate in a different way (B_3). This complex is stabilized by only two hydrogen bonds, involving two of the three nitrogen-bonded hydrogens. The H$\cdots$O distances are slightly longer than in the trimethylammonium complex (1.65 Å).

Interaction energies for these salt-bridge complexes in the gas phase were calculated as the reaction energy for the reaction

$$\left[(CH_3)_n - NH_{(4-n)}\right]^+ + CH_3COO^- \rightarrow \left[(CH_3)_n - NH^+_{(4-n)} \cdots CH_3COO^-\right], \quad (1)$$

where $n = 1$, 3 and 4.

Reaction energies range from −102.6 kcal/mol for tetramethylammonium ($n = 4$) to −133.1 kcal/mol for methylammonium ($n = 1$) (see Table 1). This strongly negative energy values are not surprising, as they lie in the expected range for charge neutralization reactions in the gas phase. Although these energies are not representative for interactions in a protein environment, they provide a basis for the discussion of the relative strength of the salt bridge interaction among ammonium compounds. The exothermicity of salt-bridge formation depends strongly on the number of nitrogen-bonded hydrogens in the ammonium compound that interact with the carboxylate oxygens of acetate. Methylammonium, with two N–H$\cdots$O bonds forms the most stable complex, while tetramethylammonium shows the weakest interaction (Table 1). Accordingly, the distance between the amine nitrogen and the carboxylate oxygen increases from 2.88 Å in methylammonium to 3.09 Å in trimethylammonium and to 3.94 Å in tetramethylammonium. The electrostatic potential maps shown in Fig. 2 indicate that in the methylammonium (B_3) and trimethylammonium (B_2) complexes the charge transfer from carboxylate to ammonium is more important than in the case of tetramethylammonium (B_1), as the electrostatic potential on the carboxylate oxygens is slightly less negative. The electrostatic potential on the methyl groups that point away from acetate is very similar in all three cases.

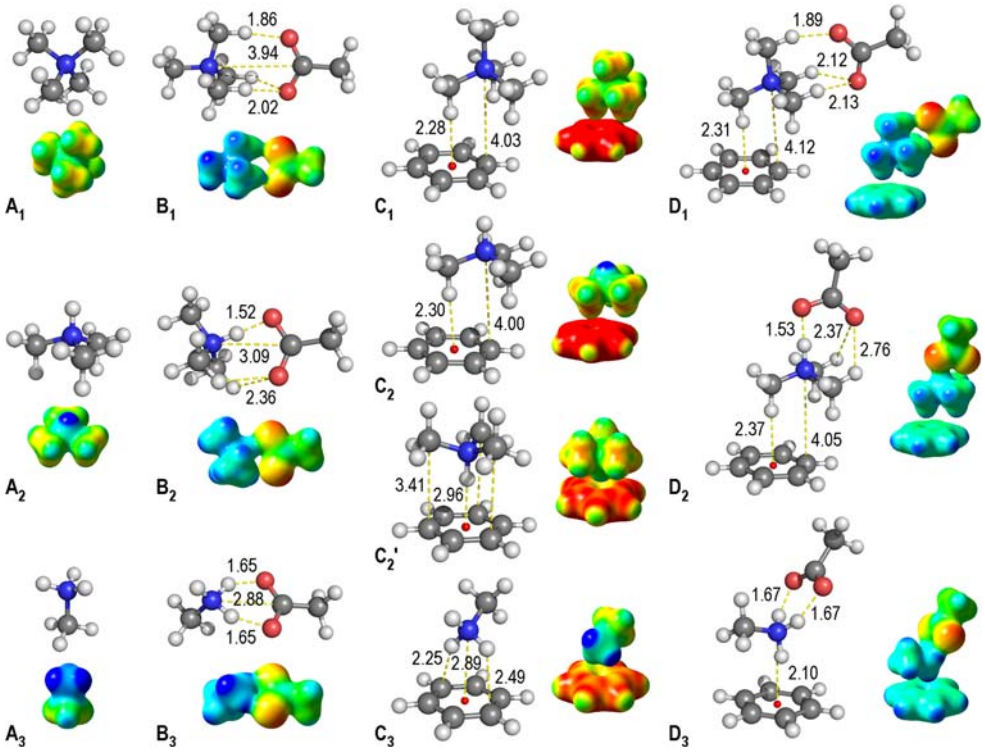

Fig. 2 MP2/aug-cc-pVDZ optimized structures and electrostatic potential surfaces of **A** amine ligands, **B** charge–charge complexes, **C** cation-π complexes and **D** combined charge–charge and cation-π complexes. Electrostatic surfaces of positive compounds A and C correspond to an energy range of +0.200 to +0.400 a.u., where blue is most positive and red least positive. Electrostatic surfaces of neutral complexes B and D correspond to an energy range of −0.125 to +0.200 a.u., where blue is positive and red is negative. All distances are given in Å

Table 1 HF/ccpVQZ solvation energies for amines in water and MP2/aug-cc-pVDZ reaction energies for the formation of cation-π, charge–charge and combined complexes (all energies in kcal/mol)

	Solvation energies	Reaction energies		
	NR_4^+(A)	$NR_4^+ + CH_3COO^-$(B)	$NR_4^+ + C_6H_6$(C)	$[NR_4^{+\cdot} CH_3COO^-] + C_6H_6$(D)
$[(CH_3)_4–N]^+$ (1)	−40.5	−102.6	−14.8	−10.6
$[(CH_3)_3–NH]^+$ (2)	−49.0	−125.0	−14.8 (C_2)	−9.2
			−23.0(C_2')	
$[CH_3–NH_3]^+$ (3)	−65.9	−133.1	−21.6	−10.8

3.3 Cation-π complexes

Highly conserved aromatic residues are found in the binding site crevice of GPCRs [12]. The fact that some of these aromatic residues are located in close vicinity to the acidic residue involved in recognition of amine ligands, suggests that they participate in ligand binding. Thus cation-π interactions are likely to form part of the interaction network in the binding site. In order to analyze the importance of aromatic residues for the binding of positively charged amine ligands, the complexes formed by tetramethylammonium $[(CH_3)_4–N]^+$, trimethylammonium $[(CH_3)_3–NH]^+$ and methylammonium $[CH_3–NH_3]^+$ with benzene $[C_6H_6]$, as a model of an aromatic side chain, were constructed (see Sect. 2). In all cases various possible conformations were optimized and the energetically most favorable are shown in Fig. 2C. In the quaternary ammonium–benzene complex (C_1) the positively charged nitrogen is placed over one of the carbon atoms in the benzene ring at a distance of 4.0 Å, while one of the methyl groups points towards the center of the ring. In contrast, the primary ammonium (C_3) interacts with benzene in a way that the nitrogen atom is positioned over the center of the ring at a distance of 2.89 Å. In the case of the tertiary ammonium interaction can take place by two different modes, with the

N–H bond pointing either away from (C_2) or towards (C'_2) the benzene ring. In the first case the coordination mode is very similar to that of the quaternary ammonium with the nitrogen center placed over one of the ring carbons at a distance of 4.0 Å, while in the second case the orientation resembles that of the primary ammonium with nitrogen placed directly over the center and the three methyl groups each placed over one of the ring carbons. The nitrogen atom is placed at 3.0 Å from the center of the ring and the methyl carbon at 3.4 Å above the nearest the ring carbon.

The interaction energy of the cation-π complexes in the gas phase (Table 1) was calculated as the reaction energy for the reaction,

$$\left[(CH_3)_n - NH_{(4-n)}\right]^+ + C_6H_6 \rightarrow \left[(CH_3)_n - NH_{(4-n)}\right]^+ \cdots C_6H_6^+, \quad (2)$$

where $n = 1$, 3 and 4.

The interaction energies for tetramethylammonium ($n = 4$) and trimethylammonium ($n = 3$), in the case that interaction with benzene takes place through the methyl groups (C_1 and C_2), are the same and amount to −14.8 kcal/mol (see Table 1). The second binding mode of trimethylammonium, in which the N–H bond points towards the benzene ring (C'_2), has a higher interaction energy (−23.0 kcal/mol). This value is close to the interaction energy of the methylammonium–benzene complex (C_1) (−21.6 kcal/mol, see Table 1), which features a similar coordination geometry. It, therefore, becomes clear that the strength of the cation-π complex depends on the manner in which the ammonium compound interacts with the π-system. The interaction is stronger when it takes place through one or more nitrogen bound hydrogens instead of methyl hydrogens. This finding can be rationalized by the different electrostatic potentials of the ammonium ligands (Fig. 2a). The N–H bonds are strongly polarized, with a significant positive charge localized on the hydrogen, which favors the interaction with the negative π-system. In contrast, the methyl groups of the substituted ammonium ligands are much less polarized, and the C–H bonds have a less positive electrostatic potential.

Clearly, the electrostatic potential of the benzene ring in the cation-π complex depends on weather the C–H groups (C_1 and C_2) or the N–H (C'_2 and C_3) of the ammonium ligand point towards the π-system. Charge transfer from the π-system to ammonium is less perceptible when interaction takes place through methyl groups. In these cases the electrostatic potential surface shows a strong negative potential on benzene (C_1 and C_2). In contrast, the interaction of one (C'_2) or more (C_3) N–H groups with benzene cause a more important charge transfer from the π-system to ammonium, which leads to a more equal charge distribution over the system. This fact shows on the electrostatic potential surface as a less negative potential on the benzene ring (C'_2 and C_3). The primary ammonium ligand $[CH_3–NH_3]^+$ forms the strongest cation-π complex with benzene (Table 1), in agreement with what was observed in the charge–charge complexes. However, the differences in energy between the different ammonium compounds are less important for cation-π than for charge–charge interactions.

3.4 Combined charge–charge and cation-π interactions

Model complexes, in which the different ammonium ligands interact simultaneously with acetate and benzene, were also energy optimized (see Sect. 2). The resulting complex structures are shown in Fig. 2D. Compared to the obtained bimolecular complexes formed by the different ammonium ligands and acetate (Fig. 2B) or benzene (Fig. 2C), all intermolecular distances are slightly lengthened. In the complexes formed by trimethylammonium (Fig. 2D_2) and methylammonium (Fig. 2D_3) acetate is located opposite of the aromatic ring. In the tetramethylammonium complex, in contrast, acetate is oriented sideways from benzene, so that the carboxylate carbon, the ammonium nitrogen and the center of the ring form an angle of 124°. The distances between the carboxylate carbon and the ring center are 7.2 Å in the tetramethylammonium complex, 7.3 Å for trimethylammonium and 5.6 Å for methylammonium. The cation-π interaction energy for ammonium with benzene in the presence of glutamate was calculated as the energy of the reaction:

$$\left[(CH_3)_n - NH^+_{(4-n)} \cdots CH_3COO^-\right] + C_6H_6 \rightarrow \left[C_6H_6 \cdots (CH_3)_n - NH^+_{(4-n)} \cdots CH_3COO^-\right], \quad (3)$$

where $n = 1$, 3 and 4.

Reaction energies for Eq. (3) are −10.6, −9.2, and −10.8 kcal/mol for tetramethylammonium (D_1), trimethylammonium (D_2), and methylammonium (D_3), respectively. These energies can be compared to the values obtained for the ammonium-benzene complex (according to Eq. 2), to evaluate the impact of the presence of acidic side chains on the cation-π interaction. The interaction of benzene with methylammonium (−21.6 kcal/mol) is 6.8 kcal/mol more exothermic than for tetramethylammonium (−14.8 kcal/mol), whereas this energy difference is negligible (0.2, −10.8 vs. −10.6 kcal/mol) in the presence of acetate. The presence of acetate triggers a charge-transfer from carboxylate to the ligand (more noticeable in methylammonium than in tetramethylammonium) and, therefore, decreases the interaction between the ligand and benzene by 10.8 kcal/mol for methylammonium (−21.6 vs. −10.8 kcal/mol) and by 4.2 kcal/mol for tetramethylammonium (−14.8 vs. −10.6 kcal/mol). The decrease in cation-π interaction energy for trimethylammonium is 5.6 kcal/mol (−9.2 vs. −14.8 kcal/mol), which is similar to the effect observed for tetramethylammonium. The

Table 2 MM-GBSA binding energy (GBTOT) (mean and SD) and its decomposition in the gas-phase (GAS) and solvation (GBSOL) terms of isoproterenol and dopamine (all energies in kcal/mol)

	Isoproterenol	Dopamine
GAS	−82.1(6.7)	−131.1(6.7)
GBSOL	61.9(5.8)	113.8(6.0)
GBTOT	−20.2(2.4)	−17.3(2.4)

second interaction mode of trimethylammonium (C'_2) was not taken into account, as in presence of acetate the most favorable interaction will always be between the N–H bond and the carboxylate oxygens.

3.5 MM-GBSA free energies of binding

The free energies of binding of isoproterenol and dopamine to the β_2AR (Table 2) have been evaluated using the MM-GBSA methodology (see Sect. 2).

These results show that both the estimated gas-phase ligand-receptor energies (GAS) and solvation energies (GBSOL) are higher in dopamine than in isoproterenol. These findings reproduce the trends found in the QM calculations, where the lower-alkyl substituted protonated amines interact stronger and have higher solvation energies (Table 1). As discussed above, this effect can be attributed to the higher charge density on the protonated amine group in lower-substituted amines (see Fig. 2A). In addition, Table 2 shows how in both ligands the GAS between ligand and receptor (−82.1 vs. −131.1 kcal/mol) is mostly used to overcome the solvation energy (GBSOL) (61.9 vs.113.8 kcal/mol), resulting in an effective binding energy (GBTOT) of −20.2 kcal/mol for isoproterenol and −17.3 kcal/mol for dopamine. Interestingly, this result also parallels the QM calculations, where, once the cation-π and solvation terms are included, higher-alkyl substituted amines have a higher interaction energy with negatively charged groups than lower-substituted amines (see Sect. 4).

4 Discussion

The ionic interaction between the alkyl-substituted protonated amine moiety of the ligand and a negatively charged amino acid side chain of the receptor is key in the process of ligand recognition. In addition, the positively charged moiety of the ligand also forms cation-π interactions with specific aromatic residues of the receptor. Therefore, the binding mode of these ligands comprises simultaneously charge–charge and cation-π interactions. In order to accurately describe the energetics of this binding mode we have performed QM calculations on model systems comprised by an alkylated protonated amine (mono-, tri- or tetramethylammonium) interacting with acetate, as a model of Asp and Glu, and benzene, as a model of aromatic side chains. As shown in Table 1, the energies of interaction of the protonated amine of the ligand with acetate and benzene are, from more negative to less negative, in the following rank order: $[CH_3–NH_3]^+$ (−133.1 and −21.6 kcal/mol), $[(CH_3)_3–NH]^+$ (−125.0 and −14.8 kcal/mol), and $[(CH_3)_4–N]^+$ (−102.6 and −14.8 kcal/mol).

According to these calculations, primary amines $[CH_3–NH_3]^+$ could be expected to bind more strongly to the receptor than higher substituted amines, since their interaction with both acetate and benzene is stronger. However, it is normally found that addition of a methyl group to the ligand, passing from a primary to a secondary amine, increases the binding affinity [62]. Thus, in addition to the energetics of the ligand-receptor complexes, additional factors must play a role. A crucial contribution to the process of ligand binding to the receptor comes from desolvation of the ligand, and has an important influence on experimentally observed binding affinities [1]. This is of special relevance in membrane proteins because the ligand has to be transferred from the extracellular aqueous environment to the binding site crevice in the transmembrane domain, frequently apart from bulk water. The energies of solvation of the differently substituted amines, as calculated quantum mechanically, are in the following rank order (see Table 1 and Sect. 2): $[CH_3–NH_3]^+$ (−65.9 kcal/mol), $[(CH_3)_3–NH]^+$ (−49.0 kcal/mol), and $[(CH_3)_4–N]^+$ (−40.5 kcal/mol). The energy needed to displace the polar primary amine $[CH_3–NH_3]^+$ from the aqueous environment to the binding pocket (65.9 kcal/mol) is therefore 16.9 kcal/mol higher than for the tertiary amine $[(CH_3)_3–NH]^+$ (49.0 kcal/mol). Once inside the binding site crevice, the interactions of the amine with carboxylate and a benzene ring are stronger for the $[(CH_3)_3–NH]^+$ than for $[CH_3–NH_3]^+$. However, the differences in interaction energy between the primary and the tertiary amine amount to only −9.6 kcal/mol (interaction with acetate is 8.1 kcal/mol stronger for $[CH_3–NH_3]^+$ than for $[(CH_3)_3–NH]^+$ and the additional interaction with a benzene ring 1.6 kcal/mol), so they cannot compensate the differences in solvation energy. Thus, the primary amine $[CH_3–NH_3]^+$ has a lower overall binding affinity than the tertiary amine $[(CH_3)_3$-$NH]^+$. The situation is different when tertiary $[(CH_3)_3–NH]^+$ and quaternary $[(CH_3)_4–N]^+$ amines are compared. Interaction with acetate is much weaker for $[(CH_3)_4–N]^+$ than for $[(CH_3)_3–NH]^+$ with a difference in energy of interaction of 22.4 kcal/mol (−102.6 kcal/mol compared to −125.0 kcal/mol). The significant decrease of 8.5 kcal/mol of the penalty of desolvation, which facilitates the entrance of $[(CH_3)_4–N]^+$ into the binding site relative to $[(CH_3)_3–NH]^+$ does not compensate the lack of interaction with acetate. However, once the ionic, charge–charge interaction is

formed, $[(CH_3)_4–N]^+$ interacts more strongly with benzene than $[(CH_3)_3–NH]^+$ (−10.6 kcal/mol compared to −9.2 kcal/mol). The stronger cation-π interaction therefore partially compensates for the weaker charge–charge interaction. Moreover, the size of the cationic quaternary $[(CH_3)_4–N]^+$ amine allows several aromatic side chains to interact with the various polar $–CH_3$ groups of the ligand. Thus, cationic quaternary amines are preferred over ternary amines to bind to a negatively charged amino acid side chain of the receptor only in the presence of several aromatic side chains. This is the case of acetylcholine esterase [9], the nicotinic acetylcholine receptor [6] or the binding of the quaternary amine moiety of TAK-779 to the chemokine CCR5 receptor [63] (see below).

The MM-GBSA calculations support the results of the quantum chemical calculations. It was found that, although the gas-phase ligand-receptor interaction energy is 49.0 kcal/mol higher for the primary amine dopamine than for the secondary amine isoproterenol, inclusion of the solvation energy inverses the trend (see Table 2). The effective binding energy, finally, is 2.9 kcal/mol higher for the secondary amine isoproterenol than for the primary amine dopamine (−20.2 vs. −17.3 kcal/mol).

We have selected the GPCR family, as an example, to further describe the influence of charge–charge and cation-π interactions on the binding of the ligand to the receptor. GPCRs recognize molecules of an extraordinary chemical and structural diversity, from odors and tastes to neurotransmitters, from peptides to ions, from hormones to a single photon [64]. In particular the ligands of amine receptors (acetylcholine, adrenergic, histamine, octopamine, dopamine, serotonin and trace amine receptors) possess a protonated amine group which interacts with a negatively charge Asp side chain in transmembrane helix 3; whereas peptides (chemokine, interleukin, and many others) possess its protonated amino terminal region that also interacts with a negatively charge Glu side chain in transmembrane helix 7.

Within the biogenic amine receptor subfamily, we have carried out a series of molecular dynamics simulations (see Sect. 2) using isoproterenol and dopamine as ligands and β_2AR as a model system. Both ligands are catecholamines, and act as a full and partial agonist, respectively, on β_2AR [47]. They have been selected due to their different degree of substitution on the protonated amine: while dopamine is a primary amine, isoproterenol presents a higher degree of substitution, having attached an extra isopropyl group. Figure 3A and 3B depict dopamine and isoproterenol in the binding pocket of a computational model of the β_2AR. The protonated amine is interacting with Asp-$113^{3.32}$ [65], the catecholic hydroxyl groups interact with Ser-$203^{5.42}$, Ser-$204^{5.43}$, Ser-$207^{5.46}$ [66,67], and the beta-hydroxyl group interacts with Asn-$293^{6.55}$ [68]. The superscripts represent the generic numbering scheme of Ballesteros and Weinstein [28] that allows easy comparison among residues in the transmembrane segments of different receptors. Interestingly, an aromatic residue Phe-$289^{6.51}$, which is a completely conserved aromatic residue in amine receptors, is close to the protonated amine group of the ligands. The interactions of the protonated amine group of the ligands and the negatively charged Asp-$113^{3.32}$ and Phe-$289^{6.51}$ are shown as yellow dashed lines in Fig. 3A and 3B. Analysis of the MD trajectories shows that the binding to the negative charge is very similar in both cases: the average distances between the N–H atom in the protonated amine group of isoproterenol and dopamine and the C_γ atom of Asp-$113^{3.32}$ are 3.7 and 3.1 Å, respectively. However, the distance from the N–H atom in the positively charged group of the ligand to the center of the aromatic ring of Phe-$289^{6.51}$ is significantly higher for isoproterenol (4.8 Å) than for dopamine (3.6 Å). As isoproterenol features a secondary amine group, each of the two amine hydrogens interact, respectively, with the negative Asp-$113^{3.32}$ and with Phe-$289^{6.51}$. This binding geometry leaves the isopropyl group available to interact with other residues of the receptor. Interestingly, the HF/6-31G*-derived RESP atomic charges of this ligand (see Sect. 2) show that the isopropyl group carries a significant partial positive charge of 0.91, so this group may be involved in additional polar or cation-π interactions. Other protonated amine moieties like piperazines are optimal to interact with $Asp^{3.32}$ and $Phe^{6.51}$ in other members of the biogenic amine subfamily like, for instance, serotonin receptors [69–71].

Chemokine receptors represent another example for GPCRs, whose ligands contain a protonated amine. While the large bulk of the chemokine binds to the extracellular part of the receptor, its amino terminal region enters the transmembrane bundle, an interaction which is known to be important for receptor activation [48,49,52,72–74]. The binding pocket of the amino terminal of chemokines is located between the extracellular ends of transmembrane helices 2, 3, 5, 6 and 7 [49] and the protonated terminal amine is supposed to interact with the negatively charged Glu$283^{7.39}$ residue, conserved in 91% of chemokine receptors [75]. Figure 3C shows the amino-terminal of MIP-1β docked into a homology model of CCR5 (see Sect. 2). The situation is similar to that in the β_2AR. Glu-$283^{7.39}$ and Trp-$86^{2.60}$ adopt an orientation pointing towards each other with the terminal amine group and the polar side chain of Ala-1 of MIP-1β positioned between them. The distance of the unsubstituted amine of MIP-1β and the carboxylate carbon of Glu-$283^{7.39}$ is 2.9 Å, while the distance between C_β of Ala-1 of MIP-1β and the center of the benzene ring of Trp-$86^{2.60}$ is 5.8 Å.

The CCR5 chemokine receptor is a co-receptor for HIV-1 entry in the cell and has therefore attracted a great amount of attention. A CCR5 inverse agonist, TAK-779, which exhibits potent anti-HIV activity [76], includes a quaternary amine in its structure (see Fig. 3D). The binding pocket for TAK-779

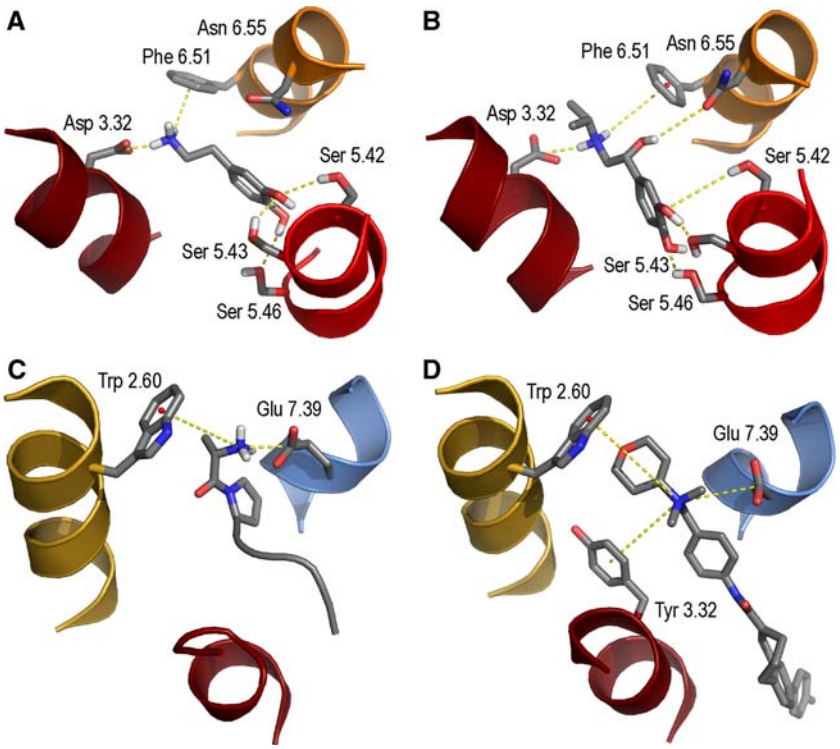

Fig. 3 Proposed interactions of the positive amine group of **A** dopamine with β_2AR, **B** isoproterenol with β_2AR, **C** the N-terminal of MIP-1β with CCR5, **D** TAK-779 with CCR5. Pictures were created with PyMOL [77]

has been mapped [63] and shows that residues involved in binding are located at the extracellular ends of transmembrane helices 1, 2, 3, 5 and 7, including the conserved Glu-283$^{7.39}$. Figure 3D shows a detail view of the binding of the quaternary amine to the receptor. The distance between the methyl carbon of the quaternary amine and the carboxylate carbon of Glu-283$^{7.39}$ is 3.2 Å. As suggested before, the multiple alkyl substituents of the cationic quaternary amine allow additional interaction with the aromatic side chains of other residues. The methyl substituents are quite polarized, as can be deduced from the HF/6-31G*-derived RESP atomic charges, which give a partial charge of 0.14 on each methyl group. In CCR5, in addition to Glu-283$^{7.39}$, the quaternary amine interacts with the aromatic side chains of Trp-86$^{2.60}$ and Tyr-108$^{3.32}$. The distance between the methyl carbons of the quaternary amine and the center of the benzene ring of Tyr-108$^{3.32}$ is 5.5 Å and the distance between the secondary carbon of the oxane group of TAK-779 and the center of the benzene ring of Trp-86$^{2.60}$ is 5.4 Å. The interaction of the cationic quaternary amine with several aromatic side chains partially compensates the weaker interaction with Glu-283$^{7.39}$. This finding could explain the fact that mutation of Glu-283$^{7.39}$ to alanine leads to only a moderate decrease in the binding affinity of TAK-779 [63]. In the absence of Glu-283$^{7.39}$ the cation-π interaction with Trp-86$^{2.60}$ and Tyr-108$^{3.32}$ may gain importance and act as a substitute for the missing charge–charge interaction.

5 Conclusions

The protonated nitrogen atom in, for instance, protonated amine ligands or N-terminal peptides, is normally involved in a charge–charge interaction with a negatively charged amino acid side chain of the receptor. This interaction is important to attract the ligand to the binding site crevice, and to provide an extra amount of binding energy to desolvate the ligand and/or trigger the conformational switches that lead to receptor activation. Importantly, alkyl groups attached to protonated amines carry a considerable positive charge and, thus, are involved in interactions with aromatic side chains of the receptor. This cation-π interaction also contributes, in a significant manner, to the binding affinity of the ligand for the receptor.

These results can be extended to other biological systems that contain negative side chain–protonated amine ligand–aromatic side chain systems.

Acknowledgements This work was supported by MEC (SAF2004-07103, SAF2006-04966), and AGAUR (SGR2005-00390).

References

1. Gohlke H, Klebe G (2002) Angew Chem Int Ed Engl 41:2644–2676
2. Dougherty DA (1996) Science 271:163–168

3. Zacharias N, Dougherty DA (2002) Trends Pharmacol Sci 23:281–287
4. Burley SK, Petsko GA (1986) FEBS Lett 203:139–143
5. Karlin S, Zuker M, Brocchieri L (1994) J Mol Biol 239:227–248
6. Ma J, Dougherty D (1997) Chem Rev 97:1303–1324
7. Singh J, Thornton JM (1990) J Mol Biol 211:595–615
8. Anderson MA, Ogbay B, Arimoto R, Sha W, Kisselev OG, Cistola DP, Marshall GR (2006) J Am Chem Soc 128:7531–7541
9. Sussman JL, Harel M, Frolow F, Oefner C, Goldman A, Toker L, Silman I (1991) Science 253:872–879
10. Beene DL, Brandt GS, Zhong W, Zacharias NM, Lester HA, Dougherty DA (2002) Biochemistry 41:10262–10269
11. Cashin AL, Petersson EJ, Lester HA, Dougherty DA (2005) J Am Chem Soc 127:350–356
12. Surgand JS, Rodrigo J, Kellenberger E, Rognan D (2006) Proteins 62:509–538
13. Fredriksson R, Lagerstrom MC, Lundin LG, Schioth HB (2003) Mol Pharmacol 63:1256–1272
14. Lander ES, Linton LM, Birren B, Nusbaum C, Zody MC, Baldwin J, Devon K, Dewar K, Doyle M, FitzHugh W, Funke R, Gage D, Harris K, Heaford A, Howland J, Kann L, Lehoczky J, LeVine R, McEwan P, McKernan K, Meldrim J, Mesirov JP, Miranda C, Morris W, Naylor J, Raymond C, Rosetti M, Santos R, Sheridan A, Sougnez C, Stange-Thomann N, Stojanovic N, Subramanian A, Wyman D, Rogers J, Sulston J, Ainscough R, Beck S, Bentley D, Burton J, Clee C, Carter N, Coulson A, Deadman R, Deloukas P, Dunham A, Dunham I, Durbin R, French L, Grafham D, Gregory S, Hubbard T, Humphray S, Hunt A, Jones M, Lloyd C, McMurray A, Matthews L, Mercer S, Milne S, Mullikin JC, Mungall A, Plumb R, Ross M, Shownkeen R, Sims S, Waterston RH, Wilson RK, Hillier LW, McPherson JD, Marra MA, Mardis ER, Fulton LA, Chinwalla AT, Pepin KH, Gish WR, Chissoe SL, Wendl MC, Delehaunty KD, Miner TL, Delehaunty A, Kramer JB, Cook LL, Fulton RS, Johnson DL, Minx PJ, Clifton SW, Hawkins T, Branscomb E, Predki P, Richardson P, Wenning S, Slezak T, Doggett N, Cheng JF, Olsen A, Lucas S, Elkin C, Uberbacher E, Frazier M, et al. (2001) Nature 409:860–921
15. Venter JC, Adams MD, Myers EW, Li PW, Mural RJ, Sutton GG, Smith HO, Yandell M, Evans CA, Holt RA, Gocayne JD, Amanatides P, Ballew RM, Huson DH, Wortman JR, Zhang Q, Kodira CD, Zheng XH, Chen L, Skupski M, Subramanian G, Thomas PD, Zhang J, Gabor Miklos GL, Nelson C, Broder S, Clark AG, Nadeau J, McKusick VA, Zinder N, Levine AJ, Roberts RJ, Simon M, Slayman C, Hunkapiller M, Bolanos R, Delcher A, Dew I, Fasulo D, Flanigan M, Florea L, Halpern A, Hannenhalli S, Kravitz S, Levy S, Mobarry C, Reinert K, Remington K, Abu-Threideh J, Beasley E, Biddick K, Bonazzi V, Brandon R, Cargill M, Chandramouliswaran I, Charlab R, Chaturvedi K, Deng Z, Di Francesco V, Dunn P, Eilbeck K, Evangelista C, Gabrielian AE, Gan W, Ge W, Gong F, Gu Z, Guan P, Heiman TJ, Higgins ME, Ji RR, Ke Z, Ketchum KA, Lai Z, Lei Y, Li Z, Li J, Liang Y, Lin X, Lu F, Merkulov GV, Milshina N, Moore HM, Naik AK, Narayan VA, Neelam B, Nusskern D, Rusch DB, Salzberg S, Shao W, Shue B, Sun J, Wang Z, Wang A, Wang X, Wang J, Wei M, Wides R, Xiao C, Yan C, et al. (2001) Science 291:1304–1351
16. Drews J (2000) Science 287:1960–1964
17. Hopkins AL, Groom CR (2002) Nat Rev Drug Discov 1:727–730
18. Imming P, Sinning C, Meyer A (2006) Nat Rev Drug Discov 5:821–834
19. Rhee MH, Nevo I, Bayewitch ML, Zagoory O, Vogel Z (2000) J Neurochem 75:2485–2491
20. Fu D, Ballesteros JA, Weinstein H, Chen J, Javitch JA (1996) Biochemistry 35:11278–11285
21. Befort K, Tabbara L, Bausch S, Chavkin C, Evans C, Kieffer B (1996) Mol Pharmacol 49:216–223
22. Peng JY, Vaidehi N, Hall SE, Goddard WA, 3rd (2006) Chem Med Chem 1:878–890
23. Wess J, Maggio R, Palmer JR, Vogel Z (1992) J Biol Chem 267:19313–19319
24. Sautel M, Rudolf K, Wittneben H, Herzog H, Martinez R, Munoz M, Eberlein W, Engel W, Walker P, Beck-Sickinger AG (1996) Mol Pharmacol 50:285–292
25. Fong TM, Cascieri MA, Yu H, Bansal A, Swain C, Strader CD (1993) Nature 362:350–353
26. Tokita K, Hocart SJ, Coy DH, Jensen RT (2002) Mol Pharmacol 61:1435–1443
27. Barroso S, Richard F, Nicolas-Etheve D, Reversat JL, Bernassau JM, Kitabgi P, Labbe-Jullie C (2000) J Biol Chem 275:328–336
28. Ballesteros JA, Weinstein H (1995) Methods Neurosci 25:366–428
29. Frisch MJ, Trucks GW, Schlegel HB, Scuseria GE, Robb MA, Cheeseman JR, Montgomery JJA, Vreven T, Kudin KN, Burant JC, Millam JM, Iyengar SS, Tomasi J, Barone V, Mennucci B, Cossi M, Scalmani G, Rega N, Petersson GA, Nakatsuji H, Hada M, Ehara M, Toyota K, Fukuda R, Hasegawa J, Ishida M, Nakajima T, Honda Y, Kitao O, Nakai H, Klene M, Li X, Knox JE, Hratchian HP, Cross JB, Bakken V, Adamo C, Jaramillo J, Gomperts R, Stratmann RE, Yazyev O, Austin AJ, Cammi R, Pomelli C, Ochterski JW, Ayala PY, Morokuma K, Voth GA, Salvador P, Dannenberg JJ, Zakrzewski VG, Dapprich S, Daniels AD, Strain MC, Farkas O, Malick DK, Rabuck AD, Raghavachari K, Foresman JB, Ortiz JV, Cui Q, Baboul AG, Clifford S, Cioslowski J, Stefanov BB, Liu G, Liashenko A, Piskorz P, Komaromi I, Martin RL, Fox DJ, Keith T, Laham MAA, Peng CY, Nanayakkara A, Challacombe M, Gill PMW, Johnson B, Chen W, Wong MW, Gonzalez C, Pople JA Gaussian 03, Revision D.01
30. Frisch MJ, Head-Gordon M, Pople JA (1990) Chem Phys Lett 166:281–289
31. Frisch MJ, Head-Gordon M, Pople JA (1990) Chem Phys Lett 166:275–280
32. Head-Gordon M, Head-Gordon T (1994) Chem Phys Lett 220:122–128
33. Head-Gordon M, Pople JA, Frisch MJ (1988) Chem Phys Lett 153:503–506
34. Saebo S, Almlof J (1989) Chem Phys Lett 154:83–89
35. Dunning TH (1989) J Chem Phys 90:1007–1023
36. Kendall RA, Dunning TH, Harrison RJ (1992) J Chem Phys 96:6796–6806
37. Peterson KA, Woon DE, Dunning TH (1994) J Chem Phys 100:7410–7415
38. Woon DE, Dunning TH (1993) J Chem Phys 98:1358–1371
39. Wilson AK, vanMourik T, Dunning TH (1996) J Mol Struct-Theochem 388:339–349
40. Cammi R, Mennucci B, Tomasi J (2000) J Phys Chem A 104:5631–5637
41. Cammi R, Mennucci B, Tomasi J (1999) J Phys Chem A 103:9100–9108
42. Tomasi J, Cammi R, Mennucci B (1999) Int J Quantum Chem 75:783–803
43. Tomasi J, Mennucci B, Cances E (1999) J Mol Struct-Theochem 464:211–226
44. Mennucci B, Cances E, Tomasi J (1997) J Phys Chem B 101:10506–10517
45. Mennucci B, Tomasi J (1997) J Chem Phys 106:5151–5158
46. Swaminath G, Deupi X, Lee TW, Zhu W, Thian FS, Kobilka TS, Kobilka B (2005) J Biol Chem 280:22165–22171
47. Yao X, Parnot C, Deupi X, Ratnala VR, Swaminath G, Farrens D, Kobilka B (2006) Nat Chem Biol 2:417–422
48. Govaerts C, Blanpain C, Deupi X, Ballet S, Ballesteros JA, Wodak SJ, Vassart G, Pardo L, Parmentier M (2001) J Biol Chem 276:13217–13225

49. Blanpain C, Doranz BJ, Bondue A, Govaerts C, De Leener A, Vassart G, Doms RW, Proudfoot A, Parmentier M (2003) J Biol Chem 278:5179–5187
50. Li J, Edwards PC, Burghammer M, Villa C, Schertler GF (2004) J Mol Biol 343:1409–1438
51. Deupi X, Olivella M, Govaerts C, Ballesteros JA, Campillo M, Pardo L (2004) Biophys J 86:105–115
52. Govaerts C, Bondue A, Springael JY, Olivella M, Deupi X, Le Poul E, Wodak SJ, Parmentier M, Pardo L, Blanpain C (2003) J Biol Chem 278:1892–1903
53. Pardo L, Deupi X, Dolker N, Lopez-Rodriguez ML, Campillo M (2007) Chembiochem 8:19–24
54. Urizar E, Claeysen S, Deupi X, Govaerts C, Costagliola S, Vassart G, Pardo L (2005) J Biol Chem 280:17135–17141
55. Jongejan A, Bruysters M, Ballesteros JA, Haaksma E, Bakker RA, Pardo L, Leurs R (2005) Nat Chem Biol 1:98–103
56. Smit MJ, Vischer HF, Bakker RA, Jongejan A, Timmerman H, Pardo L, Leurs R (2007) Annu Rev Pharmacol Toxicol 47:53–87
57. Wang J, Wolf RM, Caldwell JW, Kollman PA, Case DA (2004) J Comput Chem 25:1157–1174
58. Case DA, Darden TA, Cheatham TEI, Simmerling CL, Wang J, Duke RE, Luo R, Merz KM, Pearlman DA, Crowley M, Walker RC, Zhang W, Wang B, Hayik S, Roitberg A, Seabra G, Wong KF, Paesani F, Wu X, Brozell S, Tsui V, Gohlke H, Yang L, Tan C, Mongan J, Hornak V, Cui G, Beroza P, Mathews DH, Schafmeister C, Ross WS, Kollman PA (2006) AMBER 9, University of California, San Francisco
59. Reyes CM, Kollman PA (2000) J Mol Biol 297:1145–1158
60. Wang J, Morin P, Wang W, Kollman PA (2001) J Am Chem Soc 123:5221–5230
61. Strader CD, Sigal IS, Dixon RA (1989) Faseb J 3:1825–1832
62. Liapakis G, Chan W, Papadokostaki M, Javitch J (2004) Mol Pharmacol 65:1181–1190
63. Dragic T, Trkola A, Thompson DA, Cormier EG, Kajumo FA, Maxwell E, Lin SW, Ying W, Smith SO, Sakmar TP, Moore JP (2000) Proc Natl Acad Sci USA 97:5639–5644
64. Kristiansen K (2004) Pharmacol Ther 103:21–80
65. Strader CD, Sigal IS, Candelore MR, Rands E, Hill WS, Dixon RA (1988) J Biol Chem 263:10267–10271
66. Liapakis G, Ballesteros JA, Papachristou S, Chan WC, Chen X, Javitch JA (2000) J Biol Chem 275:37779–37788
67. Strader CD, Candelore MR, Hill WS, Sigal IS, Dixon RA (1989) J Biol Chem 264:13572–13578
68. Wieland K, Zuurmond HM, Krasel C, Ijzerman AP, Lohse MJ (1996) Proc Natl Acad Sci USA 93:9276–9281
69. Lopez-Rodriguez ML, Benhamu B, Fuente T , de la Sanz A, Pardo L, Campillo M (2005) J Med Chem 48:4216–4219
70. Lopez-Rodriguez ML, Morcillo MJ, Fernandez E, Benhamu B, Tejada I, Ayala D, Viso A, Campillo M, Pardo L, Delgado M, Manzanares J, Fuentes JA (2005) J Med Chem 48:2548–2558
71. Lopez-Rodriguez ML, Porras E, Morcillo MJ, Benhamu B, Soto LJ, Lavandera JL, Ramos JA, Olivella M, Campillo M, Pardo L (2003) J Med Chem 46:5638–5650
72. Ling K, Wang P, Zhao J, Wu YL, Cheng ZJ, Wu GX, Hu W, Ma L, Pei G (1999) Proc Natl Acad Sci USA 96:7922–7927
73. Zhou N, Luo Z, Hall JW, Luo J, Han X, Huang Z (2000) Eur J Immunol 30:164–173
74. Bondue A, Jao SC, Blanpain C, Parmentier M, LiWang PJ (2002) Biochemistry 41:13548–13555
75. Rosenkilde MM, Schwartz TW (2006) Curr Top Med Chem 6:1319–1333
76. Baba M, Nishimura O, Kanzaki N, Okamoto M, Sawada H, Iizawa Y, Shiraishi M, Aramaki Y, Okonogi K, Ogawa Y, Meguro K, Fujino M (1999) Proc Natl Acad Sci USA 96:5698–5703
77. DeLano WL (2002) The PyMOL molecular graphics system. On World Wide Web at http://www.pymol.org